

# Comparative analysis of the $^1\text{H}$ NMR relaxation enhancement produced by iron oxide and core-shell iron–iron oxide nanoparticles

O. Bomati Miguel<sup>a</sup>, Yves Gossuin<sup>b</sup>, M.P. Morales<sup>a</sup>, P. Gillis<sup>b</sup>, R.N. Muller<sup>c</sup>, Sabino Veintemillas-Verdaguer<sup>a,\*</sup>

<sup>a</sup>Department of Particulate Materials, Instituto de Ciencia de Materiales de Madrid, Cantoblanco, E 28049 Madrid, Spain

<sup>b</sup>Biological Physics Department, University of Mons-Hainaut, B 7000 Mons, Belgium

<sup>c</sup>Department of General, Organic and Biomedical Chemistry, University of Mons-Hainaut, B 7000 Mons, Belgium

Received 27 November 2006; revised 4 April 2007; accepted 13 April 2007

## Abstract

Physicochemical and magnetorelaxometric characterization of the colloidal suspensions consisting of Fe-based nanoparticles coated with dextran have been carried out. Iron oxide and iron core/iron oxide shell nanoparticles were obtained by laser-induced pyrolysis of  $\text{Fe}(\text{CO})_5$  vapours. Under different magnetic field strengths, the colloidal suspension formed by iron oxide nanoparticles showed longitudinal ( $R_1$ ) and transverse ( $R_2$ ) nuclear magnetic relaxation suspension (NMRD) profiles, similar to those previously reported for other commercial magnetic resonance imaging (MRI) contrast agents. However, colloidal suspension formed by ferromagnetic iron-core nanoparticles showed a strong increase of the  $R_1$  values at low applied magnetic fields and a strong increase of the  $R_2$  measured at high applied magnetic field. This behaviour was explained considering the larger magnetic aggregate size and saturation magnetization values measured for this sample, 92 nm and 31 emu/g Fe, respectively, with respect to those measured for the colloidal suspensions of iron oxide nanoparticles (61 nm and 23 emu/g Fe). This suspension can be used both as  $T_1$  and  $T_2$  contrast agent.

© 2007 Elsevier Inc. All rights reserved.

**Keywords:** Magnetic nanoparticles; Ferrofluids; NMR contrast agents

## 1. Introduction

Superparamagnetic colloids consisting of nanoparticles in aqueous suspensions increase the nuclear magnetic relaxation of water protons, improving the contrast in magnetic resonance imaging (MRI) [1]. These contrast media, called superparamagnetic iron oxide (SPIO) or ultrasmall superparamagnetic iron oxide (USPIO) depending on the mean aggregate size, are composed of very small iron oxide nanoparticles, usually maghemite ( $\gamma\text{-Fe}_2\text{O}_3$ ) or magnetite ( $\text{Fe}_3\text{O}_4$ ), with diameters between 3 and 10 nm, coated with a biocompatible polymer and suspended in water-based solvents [2].

Recently, the preparation of magnetic colloidal suspensions consisting of Fe-based nanoparticles prepared by laser pyrolysis and subsequently coated with dextran has been reported [3,4]. After intravenous injection of Fe metallic

core nanoparticles in rats, the contrast of in vivo  $T_2$ -weighted MRI experiments (performed at 4.7 T) was improved by 60% with respect to that obtained using an iron oxide-based commercial contrast agent (Feridex IV) [4]. The larger contrast seen on images acquired in vivo using the new Fe metallic core nanoparticles could result from several factors. Differences in the aggregating tendency and therefore in the effective size of the particles as well as the response of the liver and spleen's reticuloendothelial system to these particles could result in differences in the microscopic distribution of the agents in vivo. In addition, the different magnetic behaviour and the mechanism of proton relaxation induced by these materials in suspension could have had a significant effect on the image contrast.

The last two factors, magnetic behaviour and relaxivity, will be analysed in this work. Water proton longitudinal ( $R_1$ ) and transversal ( $R_2$ ) relaxation rate profiles (NMRD) of colloidal suspensions of iron oxide and iron core/iron oxide shell nanoparticles were measured and compared with those previously reported for other commercial iron oxide NMR

\* Corresponding author. Tel.: +34 913349061; fax: +34 913720623.

E-mail address: [sabino@icmm.csic.es](mailto:sabino@icmm.csic.es) (S. Veintemillas-Verdaguer).

contrast agents. Finally, the relation between composition and aggregate size, and the relaxation caused by these colloids will be investigated.

## 2. Materials and methods

### 2.1. Magnetic nanoparticles

Iron-based nanoparticles were synthesized by laser-induced pyrolysis of iron pentacarbonyl ( $\text{Fe}(\text{CO})_5$ ) vapours [3,4]. When air was introduced together with the carrier gas ( $\text{C}_2\text{H}_4$ ) and the iron precursor, oxidation took place subsequent to the decomposition of the  $\text{Fe}(\text{CO})_5$  and iron oxide nanoparticles were produced,  $\text{Fe}_2\text{O}_3$  [3]. However, when the system was air free, iron metal nanoparticles were obtained and a soft oxidation was only required to stabilise them against the air, giving rise to thin iron oxide layer on the iron metal cores,  $\text{Fe}@\text{Fe}_2\text{O}_3$  [4].

### 2.2. Colloidal suspensions

A suspension of 200 mg of iron nanoparticles in 2.5 ml of a 0.5 M NaOH solution was added to 2.5 ml of a 0.5 M NaOH solution containing 200 mg of dextran 6 kDa under indirect sonication, which was kept for 24 h at 30°C. After dialyses in water, the membrane (Cellu-Sep 10000 Da) was cutoff and the suspension was extracted and weighted. The obtained suspension does not settle in a month and was considered stable. In order to make it suitable for parenteral administration, the suspension was made 1 mM in tri-sodium citrate dehydrate and 5% in L-mannitol. Finally, the suspension was filtered through a 0.22- $\mu\text{m}$  pore size filter in order to make it sterile and to eliminate aggregates of potential toxicity.

### 2.3. Characterisation techniques

Iron concentration in the colloidal suspensions was determined by inductively coupled plasma spectrometry (ICP) in an emission spectrometer Plasma 40 made by Perkin Elmer. TEM was used to determine the particle size and estimate their aggregation state (JEOL-2000 FXII). The sample preparation for TEM observation was done by pulverization of the diluted sample onto a TEM grid, in order to avoid drying artefacts. Photon correlation spectroscopy (PCS) (Malvern Instruments, Zetasizer Nano S) was used to determine the mean hydrodynamic diameter of the aggregates, corresponding to the magnetic particles and the dextran coating. The hydrodynamic sizes reported in this work correspond to the maximum of the particle size distribution in volume.

The magnetic properties of the colloidal suspensions were analyzed by placing 100  $\mu\text{l}$  of the solution without dilution in a vibrating sample magnetometer VSM-NUVO from Molspin (Newcastle upon Tyne, UK). The magnetization was recorded over a field range of  $-5$  to  $5$  T at 298 K, and the values were normalized by the iron content to yield specific magnetization ( $\text{emu/g Fe}$ ).

Water proton longitudinal relaxation time ( $T_1$ ) and  $R_1$ -NMRD profiles as function of the static magnetic field were performed by using a Spinmaster fast field cycling relaxometer (STELAR, Mede, Italy) working at Larmor proton frequencies ( $\nu_0$ ) from 0.01 to 10 MHz (a proton Larmor frequency of 10 MHz corresponds to a magnetic field of 0.24 T) and  $T=37^\circ\text{C}$ . The uncertainty of this measurement was less than 3%. The experimental  $R_1$  values were fitted by using a theoretical model developed by Roch et al. [1,5] for proton relaxation induced by superparamagnetic nanoparticles.

The field dispersion of the transverse relaxation time,  $T_2$  and  $T_1$  values beyond 10 MHz was measured by means of four low-field Minispec BRUKER PC110 PC120, PC140 and mq60 spectrometers working at Larmor proton frequencies of 10, 20, 40 and 60 MHz, respectively, and  $T=37^\circ\text{C}$ . In addition, high-field measurements were performed on a BRUKER AMX 300 (300 MHz) spectrometer.  $T_1$  was determined with an inversion-recovery sequence, and  $T_2$  measurements were carried out by using a Carr-Purcell-Meiboom-Gill sequence (CPMG), with an echo time (TE) of 1 ms for all measurements and a repetition time (TR) always longer than  $5 T_1$ .

## 3. Results and discussion

Stable colloidal suspensions of iron oxide ( $\text{Fe}_2\text{O}_3$ ) and iron-core ( $\text{Fe}@\text{Fe}_2\text{O}_3$ ) nanoparticles in water at pH 7 were obtained after coating with dextran. The final iron concentration was different for both samples in order to obtain stable suspensions. ICP measurements found Fe concentration of 185 and 21.1 mM for samples  $\text{Fe}_2\text{O}_3$  and

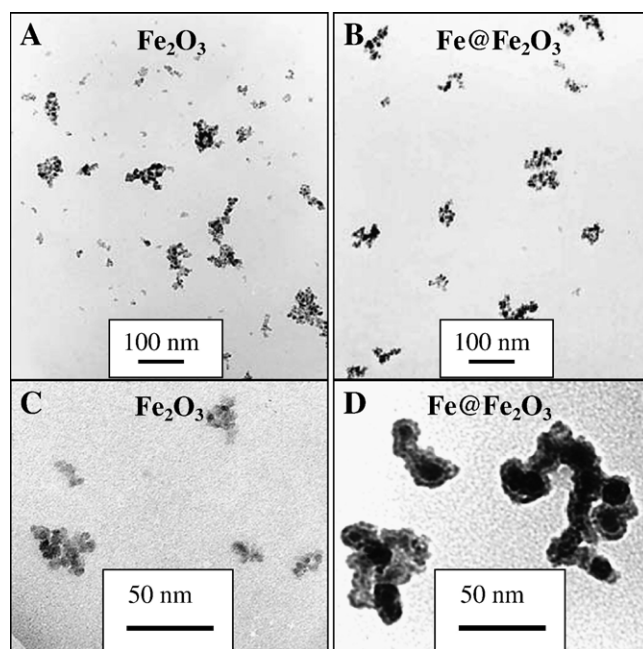


Fig. 1. TEM images of the nanoparticle aggregates present in the iron oxide ( $\text{Fe}_2\text{O}_3$ ) and iron-core ( $\text{Fe}@\text{Fe}_2\text{O}_3$ ) suspensions.

Table 1

Morphological and magnetic properties of powders and suspensions based on iron oxide and iron-core nanoparticles coated with dextran

Sample	Powders				Suspensions	
	Crystal size (DRX) (nm)	Particle size (TEM) (nm)	Magnetic properties RT		Aggregate size	
			Ms (emu/g Fe)	H (Oe)	$D_{\text{TEM}}$ (nm)	$D_{\text{PCS}}$ (nm)
Fe <sub>2</sub> O <sub>3</sub>	3.2	3.5	41	0	25	61
Fe@Fe <sub>2</sub> O <sub>3</sub>	7.0	12	83	400	52	92

Fe@Fe<sub>2</sub>O<sub>3</sub>, respectively. Due to dipolar interactions, the sample having nanoparticles with a metal core partially developed aggregates if the concentration is higher than the above-mentioned.

TEM images of the colloidal suspensions showed the presence of uniform nanoparticulate aggregates (Fig. 1A and B). The mean aggregate diameters obtained by TEM ( $D_{\text{TEM}}$ ) were 25 and 52 nm, while PCS yielded hydrodynamic size of colloidal aggregates ( $D_{\text{PCS}}$ ) of 61 and 92 nm for samples Fe<sub>2</sub>O<sub>3</sub> and Fe@Fe<sub>2</sub>O<sub>3</sub> respectively (Table 1). From the differences between  $D_{\text{PCS}}$  and  $D_{\text{TEM}}$  values, a thickness of the hydrated dextran layer of about 20 nm was

inferred. The aggregate size is a consequence of both, the nature and the mean size of the particles (Table 1). Thus, TEM mean particle size goes from  $3.5 \pm 2$  nm for sample Fe<sub>2</sub>O<sub>3</sub> to  $12 \pm 4$  nm for sample Fe@Fe<sub>2</sub>O<sub>3</sub>, in good agreement with the crystal sizes obtained by X-ray diffraction (Table 1). The structure of the aggregates is shown in Fig. 1C and D. In the case of sample Fe@Fe<sub>2</sub>O<sub>3</sub>, a core/shell structure consisting of a  $\alpha$ -Fe core and an oxide layer is clearly shown in Fig. 1D. Core/shell structure is absent in the homogeneous Fe<sub>2</sub>O<sub>3</sub> nanoparticles (Fig. 1C). It should be noted that the mean hydrodynamic size values obtained for both suspensions were similar to those measured for a typical SPIO commercial contrast agents such as ENDOREM ( $D_{\text{PCS}}=73$  nm). Therefore, the colloidal suspensions obtained in this work can be classified within the contrast agents called SPIO (mean size >50 nm) [2].

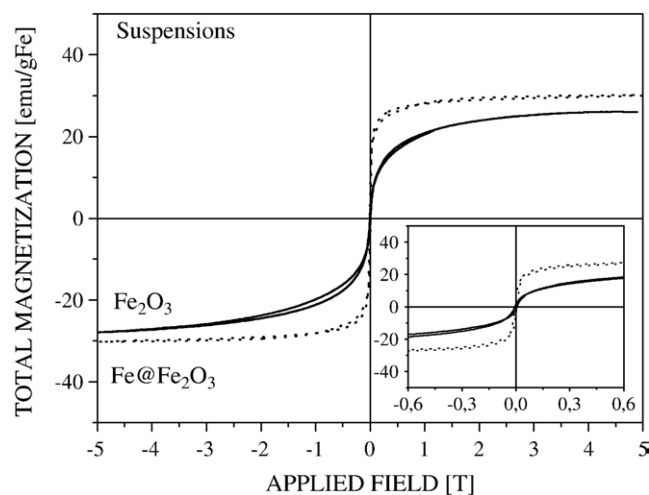
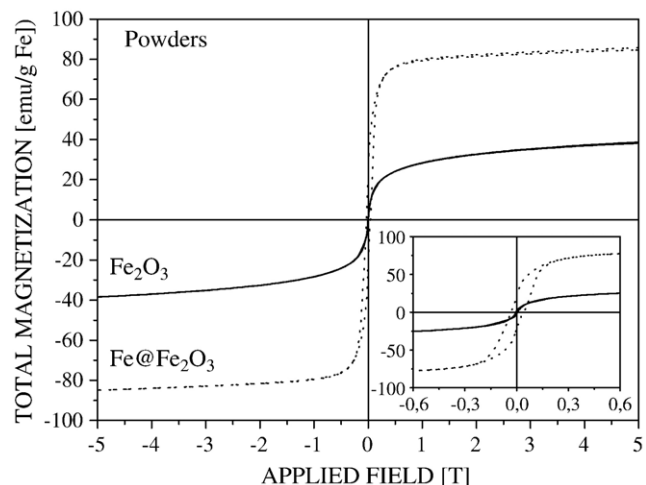


Fig. 2. Magnetization curves at room temperature for powders and suspensions of iron oxide and iron-core nanoparticles.

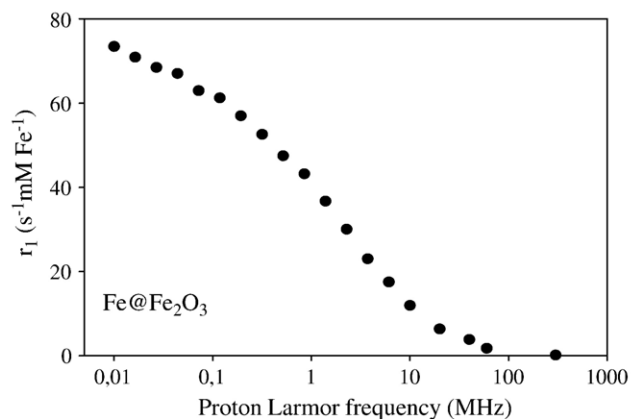
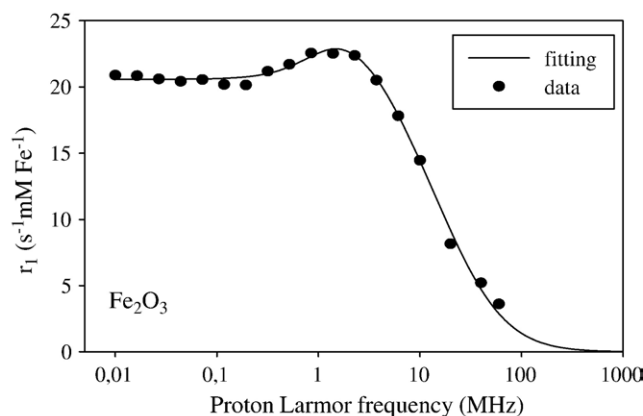


Fig. 3.  $R_1$ -NMRD profiles for suspensions of iron oxide and iron-core nanoparticles.

Magnetic hysteresis curves for the iron oxide powder and their suspensions show superparamagnetic behaviour at room temperature (Fig. 2). Iron-core nanoparticles in powder form presented ferromagnetic behaviour with detectable coercivity at room temperature (Table 1). In the colloidal state, the dispersions produced by these iron-core nanoparticles behave as superparamagnetic (Fig. 2). This quasi-superparamagnetic behaviour according to previous studies was attributed to Brownian motion of the noninteracting magnetic aggregates, i.e., free rotation of the magnetization in the liquid. The  $M_s$  for the suspensions estimated by fitting the magnetization curve with a Langevin function was found to be 26.5 and 31 emu/g Fe for samples  $\text{Fe}_2\text{O}_3$  and  $\text{Fe}@\text{Fe}_2\text{O}_3$  respectively. These results seem to indicate the important influence of the structure of the aggregates on the magnetic response of the colloidal suspensions under the influence of an applied magnetic field. Insets in Fig. 2 show that above 0.3 T, powder and suspension of the iron-core sample are almost saturated, while for the iron oxide nanoparticles, the magnetization at this field is half of the saturation value.

The magnetic field dependence of the  $R_1$ -NMRD profile for sample  $\text{Fe}_2\text{O}_3$  was characterized by the presence of a low-field plateau, a peak at about 2 MHz, and a final decrease to zero at high fields (or high Larmor frequencies) (Fig. 3). The peak is caused by the increase of the magnetization and successive alignment of the particle magnetic moments derived from the increase of magnetic field [5,6]. The parameters generated by the fitting of the  $R_1$ -NMRD profile using a previously developed model [5] gave us the following information about the particles: saturation magnetization, 23 emu/g Fe; the radius of the crystal, 9.1 nm; and the Néel relaxation time, 35.4 ns. On the other hand, the  $R_1$ -NMRD experimental curve for sample  $\text{Fe}@\text{Fe}_2\text{O}_3$  showed bigger values of the longitudinal relaxivity at low fields with a strong decrease to zero as the applied magnetic field increases (Fig. 3). The theoretical model developed for pure superparamagnetic particles in Ref. [5] was not applicable in this case due to the larger aggregate size for the  $\text{Fe}@\text{Fe}_2\text{O}_3$  particles and their complex composition.

Fig. 4 shows the transverse relaxivity ( $R_2$ ) recorded from 20 to 300 MHz (0.47–7 T) for samples  $\text{Fe}_2\text{O}_3$  and  $\text{Fe}@\text{Fe}_2\text{O}_3$ . In both cases, the transverse relaxivity seems to reach a constant value at high applied fields, similar to that reported for ENDOREM [2]. In addition, a strong increase of the transverse relaxation at high applied field was detected from sample  $\text{Fe}@\text{Fe}_2\text{O}_3$  with respect to sample  $\text{Fe}_2\text{O}_3$ . The obtained values were in the same order as or higher than those reported for commercial SPIO suspensions (ENDOREM),  $R_1=24 \text{ s}^{-1} \text{ mM}^{-1}$  and  $R_2=107 \text{ s}^{-1} \text{ mM}^{-1}$  at  $37^\circ\text{C}$  and 20 MHz [7]. According to Roch et al. [1], the higher values of  $R_2$  observed for sample  $\text{Fe}@\text{Fe}_2\text{O}_3$  can be attributed to the higher magnetic moment of the individual particle and the increase of the aggregate size. In any case, the high value of  $R_2$  obtained can justify the higher contrast

obtained in the MRI images using aqueous dispersions of these particles [4].

The plateau observed in the  $R_2$ -NMRD profiles for  $\text{Fe}_2\text{O}_3$  and  $\text{Fe}@\text{Fe}_2\text{O}_3$  was predicted by the theory [1], but it was not observed previously due to the surface paramagnetic contribution [1,8]. We suggest that this paramagnetic component is only present when the magnetic nanoparticles are synthesized by coprecipitation of Fe (III)+Fe (II) salts. This contribution is not present in the laser pyrolysis samples obtained from iron pentacarbonyl decomposition in gas phase and in situ oxidation of the iron particles initially formed [3,4].

#### 4. Conclusion

Pharmaceutical grade colloidal suspensions (SPIO) have been obtained from very uniform iron oxide and iron-core nanoparticles prepared by laser pyrolysis. The colloidal suspension formed from iron-core nanoparticles shows an increase of the transverse relaxation rate resulting from the larger mean aggregate size and larger values of saturation magnetization. Additionally, these suspensions can, in principle, be used as a  $T_1$  contrast agent, in applications when extravasations of small gadolinium complexes are a disadvantage. Based on their larger relaxivities, this material

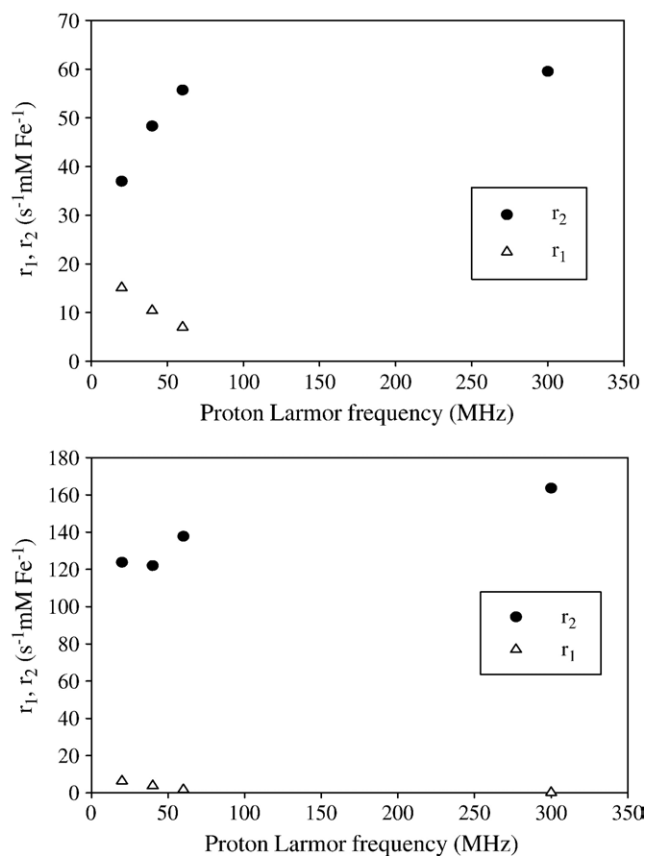


Fig. 4.  $R_2$ -NMRD profiles for suspensions of iron oxide and iron-core nanoparticles.  $R_1$  values are included for comparison.

seems to be very promising for developing more efficient contrast agents for MRI.

### Acknowledgments

This work was supported by the Accion Estratégica de Nanociencia y Nanotecnología 2004-2007 program of the Spanish Education Ministry (project no. NAN2004-08805-CO4-01) and by the Community of Madrid (project no. S-0505/MAT/0194).

### References

- [1] Roch A, Gossuin Y, Muller RN, Gillis P. Superparamagnetic colloid suspensions: water magnetic relaxation and clustering. *J Magn Mater* 2005;293:532–9.
- [2] Muller RN, Roch A, Colet J-M, Ouakssim A, Gillis P. Particulate magnetic contrast agents. In: Merbach AE, Tóth E, editors. The chemistry of contrast agents in medical magnetic resonance imaging. Chichester: John Wiley & Sons Ltd; 2001. p. 417–35.
- [3] Veintemillas-Verdaguer S, Morales MP, Bomati-Miguel O, Bautista C, Zhao X, Bonville P, et al. Colloidal dispersions of maghemite nanoparticles produced by laser pyrolysis with application as NMR contrast agents. *J Phys D: Appl Phys* 2004;37:2054–9.
- [4] Bomati-Miguel O, Morales MP, Tartaj P, Ruiz-Cabello J, Bonville P, Santos M, et al. Fe-based nanoparticulate metallic alloys as contrast agents for magnetic resonance imaging. *Biomaterials* 2005; 26:5695–703.
- [5] Roch A, Muller RN, Gillis P. Theory of proton relaxation induced by superparamagnetic particles. *Chem Phys* 1999;110:5403–11.
- [6] Bulte JW, Vymazal J, Brooks RA, Pierpaoli C, Frank JA. Frequency dependence of MR relaxation times: II. Iron oxides. *J Magn Reson Imaging* 1993;3:641–8.
- [7] Merbach E, Tóth E, editors. The chemistry of contrast agents in medical magnetic resonance imaging. Chichester (UK): John Wiley & Sons; 2001.
- [8] Bulte JW, Brooks RA, Moskowitz BM, Bryant LH, Frank JA.  $T_1$  and  $T_2$  relaxometry of monocrystalline iron oxide nanoparticles (MION-46L): theory and experiment. *Acad Radiol* 1998;5:S137–40.